

**A GLOBAL NUMERICAL WEATHER PREDICTION MODEL WITH VARIABLE RESOLUTION.  
APPLICATION TO THE SHALLOW-WATER EQUATIONS**

Philippe Courtier  
European Centre for Medium Range Weather Forecasts  
Reading, United Kingdom

and

Jean-François Geleyn  
Direction de la Météorologie  
Paris, France

1. INTRODUCTION

One of the weaknesses of current global numerical weather prediction models is that the horizontal resolution is too coarse for the representation of the local weather. For example, the half wavelength of the shortest wave represented in the operational T106 ECMWF model is 190 km; even at truncation T159, the finest resolution currently possible in research mode at ECMWF, it is still 125 km. On the other hand, limited area models allow the treatment of shorter waves but they present problems linked with the treatment of the lateral boundary conditions.

As the sphere itself is a limited area, people have been looking for a long time for solutions which combine the advantages of the above two approaches. One obvious way in a grid point model is to have a variable mesh with a sufficient concentration of grid points in the area of interest and lower resolution outside, though still enough for resolving the synoptic waves.

The difficulty with such a solution is that, due to the variation of resolution, reflection and refraction of waves occurs. At a more fundamental level, the local interactions are no longer isotropic: the derivative in one direction and in another one do not involve the same scales.

Ten or so years ago, F. Schmidt (1977) proposed a clean solution to define a global variable mesh model with local isotropic interactions. One defines a transformation from the earth to another sphere and discretizes the equations on the latter sphere. If the transformation is conformal (angle-preserving) then the local interactions are effectively isotropic. He proposed a transformation which gives an area of concentration, and one of dilation at

the antipode. It is important to realize here that what happens, after this transform, to classical shallow water (or primitive) equations is, but for a few technical details, the mere introduction of a local map factor with the associated change of wind variables. Anybody having worked with models on a polar stereographic projection is of course familiar with this presentation and should feel at ease with the use of this transformation, provided he accepts to think in terms of the transformed earth (see example figure 1), a representation no more and no less deforming than the usual polar stereographic projection but less customary, up to now.

Once the transformation is defined, it is possible to use either isotropic spectral or grid-point discretizations on the transformed sphere. However the method seems particularly suitable for the spectral discretization since an isotropic discretization on the transformed sphere is achieved by the choice of a triangular truncation.

In section 2 we prove the uniqueness of the transformation introduced by Schmidt using differential geometry (it is repeated with classical geometry in Appendix A for readers with a different taste). In section 3 we present the implementation in a shallow water equation model with semi implicit time integration scheme and non linear normal mode initialization. Numerical results in section 4 demonstrate the feasibility of the method and application in the operational and research context are discussed in section 5.

## 2. THE TRANSFORMATION

### 2.1 The problem

Let us consider a mapping  $f$  of the sphere  $\Omega$  of radius 1 defined by:

$$(\lambda', \mu') = f(\lambda, \mu) \quad (2.1)$$

where  $\mu$  is the sine of the latitude,  $\lambda$  the longitude and the prime denote the system of coordinates on the mapped sphere. As noted by Schmidt (1977), the shallow-water equations can be expressed in terms of three differential operators:

$$\begin{aligned} \tilde{\nabla}_A \times \tilde{\nabla}_B &= \frac{\partial A}{\partial \lambda} \frac{\partial B}{\partial \mu} - \frac{\partial A}{\partial \mu} \frac{\partial B}{\partial \lambda} \\ \tilde{\nabla}_A \cdot \tilde{\nabla}_B &= \frac{1}{1-\mu^2} \frac{\partial A}{\partial \lambda} \frac{\partial B}{\partial \lambda} + (1-\mu^2) \frac{\partial A}{\partial \mu} \frac{\partial B}{\partial \mu} \\ \nabla^2 A &= \Delta A = \frac{\partial}{\partial \mu} \left( (1-\mu^2) \frac{\partial A}{\partial \mu} \right) + \frac{1}{1-\mu^2} \frac{\partial^2 A}{\partial \lambda^2} \end{aligned} \quad (2.2)$$



Fig. 1 Transformed Earth ( $c=4$ ) seen from infinity.

where  $\nabla$  is the first order differential operator over the sphere  $\Omega$  and A and B two scalar fields. "." denotes the scalar product of two horizontal vectors and "x" the two dimensional vectorial product (vertical component of the three dimensional vectorial product of two horizontal vectors). If  $f$  is a conformal mapping (i.e. fulfils the Cauchy-Riemann condition as expressed by Schmidt, 1977), then we have the remarkable property:

$$\begin{aligned}\nabla A \times \nabla B &= \nabla' A' \times \nabla' B' \cdot F'(\lambda', \mu') \\ \nabla A \cdot \nabla B &= \nabla' A' \cdot \nabla' B' \cdot F'(\lambda', \mu') \\ \nabla^2 A &= \nabla'^2 A' \cdot F'(\lambda', \mu')\end{aligned}\tag{2.3}$$

where  $\nabla'$  is the first order differential operator with respect to the transformed coordinates  $(\lambda', \mu')$  and A' and B' the fields A and B considered as functions of  $(\lambda', \mu')$ . The so called mapping factor,  $F'(\lambda', \mu')$  is (with the choice of  $(\lambda, \mu)$  as the system of coordinates), the determinant of the plane Jacobian matrix of the mapping  $f$ :

$$F'(\lambda', \mu') = \begin{vmatrix} \frac{\partial \lambda'}{\partial \lambda} & \frac{\partial \mu'}{\partial \lambda} \\ \frac{\partial \lambda'}{\partial \mu} & \frac{\partial \mu'}{\partial \mu} \end{vmatrix} = \begin{vmatrix} \frac{\partial \lambda}{\partial \lambda'} & \frac{\partial \mu}{\partial \lambda'} \\ \frac{\partial \lambda}{\partial \mu'} & \frac{\partial \mu}{\partial \mu'} \end{vmatrix}^{-1}\tag{2.4}$$

The fundamental remark which makes feasible the spectral method using a collocation grid with no aliasing errors for the shallow-water equations is that if at a given instant, the vorticity, divergence and geopotential are expressed in finite series of spherical harmonics, then the tendencies of those fields are also expressed in finite series of spherical harmonics. Due to the quadratic terms, the maximum degree of the tendencies is twice that of the fields (Jarraud and Simmons, 1983).

This property is conserved in the shallow-water equations transformed by a conformal mapping (the fields and the Coriolis parameter being expressed in finite series of spherical harmonics defined over the mapped sphere) if and only if the function  $F'(\lambda', \mu')$  has a decomposition in a finite set of spherical harmonics of the mapped sphere. The mapping is then said to be spectral. Furthermore, the lower the order of this decomposition, the less additional degrees of freedom the collocation grid will require.

In the following, we shall identify all the conformal mapping of the sphere using a classical result of holomorphic functions, and then identify all the spectral mappings.

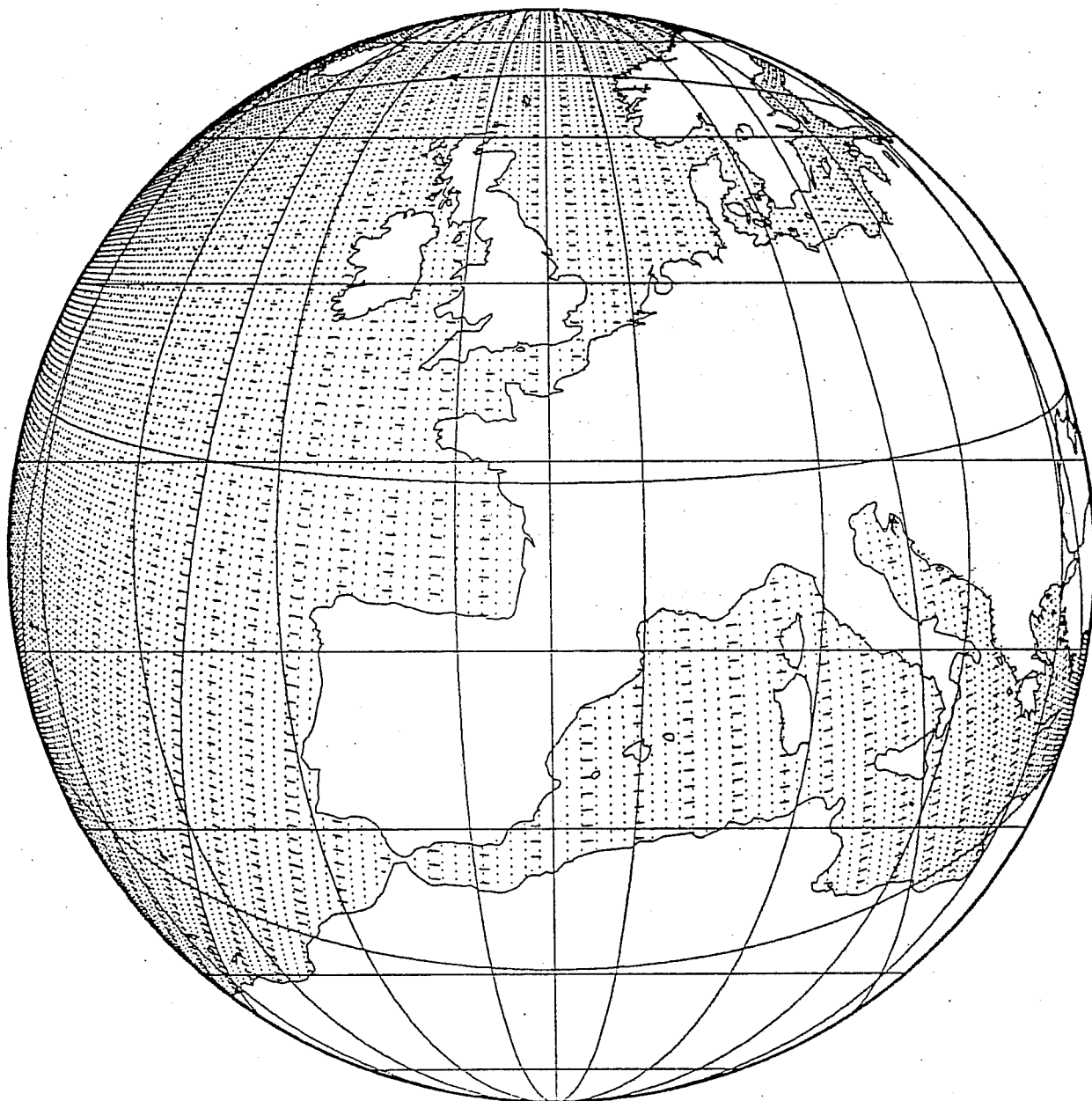


Fig. 1 Transformed Earth ( $c=4$ ) seen from infinity.

where  $\nabla$  is the first order differential operator over the sphere  $\Omega$  and A and B two scalar fields. "." denotes the scalar product of two horizontal vectors and "x" the two dimensional vectorial product (vertical component of the three dimensional vectorial product of two horizontal vectors). If  $f$  is a conformal mapping (i.e. fulfils the Cauchy-Riemann condition as expressed by Schmidt, 1977), then we have the remarkable property:

$$\begin{aligned}\nabla A \times \nabla B &= \nabla' A' \times \nabla' B' \cdot F'(\lambda', \mu') \\ \nabla A \cdot \nabla B &= \nabla' A' \cdot \nabla' B' \cdot F'(\lambda', \mu') \\ \nabla^2 A &= \nabla'^2 A' \cdot F'(\lambda', \mu')\end{aligned}\tag{2.3}$$

where  $\nabla'$  is the first order differential operator with respect to the transformed coordinates  $(\lambda', \mu')$  and A' and B' the fields A and B considered as functions of  $(\lambda', \mu')$ . The so called mapping factor,  $F'(\lambda', \mu')$  is (with the choice of  $(\lambda, \mu)$  as the system of coordinates), the determinant of the plane Jacobian matrix of the mapping  $f$ :

$$F'(\lambda', \mu') = \begin{vmatrix} \frac{\partial \lambda'}{\partial \lambda} & \frac{\partial \mu'}{\partial \lambda} \\ \frac{\partial \lambda'}{\partial \mu} & \frac{\partial \mu'}{\partial \mu} \end{vmatrix} = \begin{vmatrix} \frac{\partial \lambda}{\partial \lambda'} & \frac{\partial \mu}{\partial \lambda'} \\ \frac{\partial \lambda}{\partial \mu'} & \frac{\partial \mu}{\partial \mu'} \end{vmatrix}^{-1}\tag{2.4}$$

The fundamental remark which makes feasible the spectral method using a collocation grid with no aliasing errors for the shallow-water equations is that if at a given instant, the vorticity, divergence and geopotential are expressed in finite series of spherical harmonics, then the tendencies of those fields are also expressed in finite series of spherical harmonics. Due to the quadratic terms, the maximum degree of the tendencies is twice that of the fields (Jarraud and Simmons, 1983).

This property is conserved in the shallow-water equations transformed by a conformal mapping (the fields and the Coriolis parameter being expressed in finite series of spherical harmonics defined over the mapped sphere) if and only if the function  $F'(\lambda', \mu')$  has a decomposition in a finite set of spherical harmonics of the mapped sphere. The mapping is then said to be spectral. Furthermore, the lower the order of this decomposition, the less additional degrees of freedom the collocation grid will require.

In the following, we shall identify all the conformal mapping of the sphere using a classical result of holomorphic functions, and then identify all the spectral mappings.

## 2.2 The conformal mappings of the sphere

We call  $P'$  the complex plane  $P$  to which we add the infinite point. The sphere is then classically identified to  $P'$  using the polar stereographic projection ( $P'$  is called the Riemann sphere). Then a classical result is that all the conformal mappings of  $P'$  are given by the homographic transformations (also called bilinear, linear fractional or Möbius transformations) (Cartan, 1961), see also (Saff and Snider, 1976) for an English reference. We consider only transformations which preserve also the sign of the angle, we have thus excluded the inversion (symmetry with respect to a plane containing a great circle). There is no loss of generality since the transformations which preserve the angle but not the sign are either holomorphic in  $z$  or in its conjugate  $\bar{z}$ . The homographic transformations have the form:

$$h(z) = \frac{\alpha z + \beta}{\gamma z + \delta} \quad (z \quad , \quad \alpha\delta - \beta\gamma \neq 0) \quad (2.5)$$

which corresponds to six degrees of freedom.

We can easily see that this transformation has two fixed points (or one double). We make a rotation of the sphere in such a way that the southern pole (the infinite point in  $P'$ ) is invariant in the transformation. Since all the conformal transformations of the complex plan  $P$  are the similarities,  $h$  reduces to the form:

$$h(z) = c(z + be^{i\tau}) \quad (2.6)$$

The transformation  $z \rightarrow z e^{i\tau}$  is a rotation around the polar axis, so we can assume with no loss of generality that  $c$  is real positive.  $h(z) = c z$  is the magnification of ratio  $c$  and centre the origin (northern pole) and  $h(z) = z + be^{i\tau}$  is the translation of vector  $be^{i\tau}$ .

All the conformal mappings of the sphere  $\Omega$  can be decomposed into the product of rotations (the three Euler angles corresponds to three degrees of freedom) and of two elementary transformations of the Riemann sphere  $P'$  (one degree of freedom for the magnification and two for the translation). The rotations do not change the resolution over the sphere and their associated mapping factor is constant and equal to one.

The magnification is the transformation identified by Schmidt, 1977, for which he proved that it is spectral. We shall prove that the translations are spectral.

### 2.3 The translations are spectral

We consider the translation  $h(z) = z + be^{i\tau}$  where  $\tau$  is assumed equal to zero for convenience (translation parallel to the real axis). We then express the associated mapping  $f$  of the sphere  $\Omega: (\lambda', \mu') = f(\lambda, \mu)$ . (See Figure 2).

Let  $(r, \theta)$  be the polar coordinates in the complex plane. We have:

$$\mu = \frac{4-r^2}{4+r^2} \quad \lambda = \theta \quad r^2 = 4 \frac{1-\mu}{1+\mu} \quad (2.7)$$

The transformation is then:

$$(\lambda, \mu) \rightarrow re^{i\theta} \rightarrow r\cos\theta + b + ir\sin\theta \rightarrow (\lambda', \mu')$$

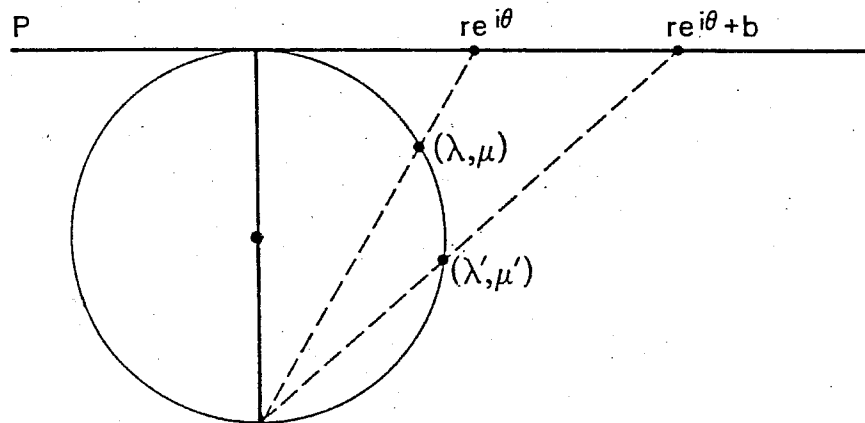


Fig. 2 The transformation associated to a translation in the complex plane.

$(\lambda', \mu')$  are then related to  $(\lambda, \mu)$  by:

$$\tan(\lambda') = \frac{2\sqrt{1-\mu}\sin\lambda}{2\sqrt{1-\mu}\cos\lambda + b\sqrt{1+\mu}} \quad (2.8)$$

$$\mu' = \frac{8\mu - b^2(1+\mu) - 4b\sqrt{1-\mu^2}\cos\lambda}{8 + b^2(1+\mu) + 4b\sqrt{1-\mu^2}\cos\lambda}$$



The inverse transform is obtained from a translation of  $(-b)$ , so we have:

$$\tan(\lambda) = \frac{2 \sqrt{1-\mu'} \sin \lambda'}{2 \sqrt{1-\mu'} \cos \lambda' - b\sqrt{1+\mu'}} \quad (2.9)$$

$$\mu = \frac{8 \mu' - b^2 (1+\mu') + 4b\sqrt{1-\mu'^2} \cos \lambda'}{8 + b^2(1+\mu') - 4b\sqrt{1-\mu'^2} \cos \lambda'}$$

The partial derivatives involved in the mapping factor are found to be:

$$\begin{aligned} \frac{\partial \mu}{\partial \mu'} &= 32 \frac{(2 - b \cos \lambda' \sqrt{\frac{1+\mu'}{1-\mu'}})}{(8 - 4b \sqrt{1-\mu'^2} \cos \lambda' + b^2 (1+\mu'))^2} \\ \frac{\partial \mu}{\partial \lambda'} &= 32 \frac{-b (\mu'+1) \sqrt{1-\mu'^2} \sin \lambda'}{(8-4b \sqrt{1-\mu'^2} \cos \lambda' + b^2 (1+\mu'))^2} \\ \frac{\partial \lambda}{\partial \lambda'} &= 2 \frac{(2(1-\mu') - b \cos \lambda' \sqrt{1-\mu'^2})}{4(1-\mu') - 4b\sqrt{1-\mu'^2} \cos \lambda' + b^2(1+\mu')} \\ \frac{\partial \lambda}{\partial \mu'} &= 2 \frac{b \sin \lambda'}{\sqrt{1-\mu'^2} (4(1-\mu') - 4b\sqrt{1-\mu'^2} \cos \lambda' + b^2(1+\mu'))} \end{aligned} \quad (2.10)$$

and the mapping factor is then:

$$F'(\lambda', \mu') = \frac{(8 - 4b\sqrt{1-\mu'^2} \cos \lambda' + b^2(1+\mu'))^2}{64} \quad (2.11)$$

If the translation is of vector  $be^{i\tau}$  where  $b$  and  $\tau$  are real numbers, by performing a rotation of the cartesian referential of angle  $\tau$  and applying the previous result, we have the mapping factor:

$$F'(\lambda', \mu') = \frac{(8 - 4b\sqrt{1-\mu'^2} \cos(\lambda'-\tau) + b^2(1+\mu'))^2}{64} \quad (2.12)$$

The mapping factor is the square of a sum of spherical harmonics of degree 0 and 1, defined over the transformed sphere so it is of degree 2, so the translations are spectral.

#### 2.4 The homotheties are spectral

We study the mappings associated to the transformations  $f(z) = cz$  of the Riemann sphere  $P'$  where  $c$  is real. The transformation is:

$$(\lambda, \mu) \rightarrow re^{i\theta} + cre^{i\theta} \rightarrow (\lambda', \mu')$$

we have:

$$\lambda' = \theta = \lambda \quad (2.13)$$

$$\mu' = \frac{4 - c^2 r^2}{4 + c^2 r^2} = \frac{1 - c^2 + \mu(1 + c^2)}{1 + c^2 + \mu(1 - c^2)}$$

the inverse transform is obtained for  $c^{-1}$ , so we have:

$$\mu = \frac{c^2 - 1 + \mu'(1 + c^2)}{1 + c^2 + \mu'(c^2 - 1)} \quad (2.14)$$

the partial derivatives are then:

$$\begin{aligned} \frac{\partial \lambda}{\partial \lambda'} &= 1 \\ \frac{\partial \lambda}{\partial \mu'} &= 0 \\ \frac{\partial \mu}{\partial \lambda'} &= 0 \\ \frac{\partial \mu}{\partial \mu'} &= \frac{4 c^2}{(1 + c^2 + \mu'(c^2 - 1))^2} \end{aligned} \quad (2.15)$$

and the mapping factor:

$$F'(\lambda', \mu') = \frac{(1 + c^2 + \mu'(c^2 - 1))^2}{4 c^2} \quad (2.16)$$

It is the square of a Legendre polynomial of degree 1, so in terms of spherical harmonics, its degree is 2.

## 2.5 The transformation $z \rightarrow c(z + be^{i\tau})$ is spectral and of degree 2

This transformation is the composition of a homothetic H and a translation T.

We have:

$$(\lambda, \mu) \xrightarrow{T} (\lambda', \mu') \xrightarrow{H} (\lambda'', \mu'')$$

The mapping factor is the product of the mapping factors of T and H. We have:

$$\begin{aligned} F'(\lambda'', \mu'') &= \frac{(8 - 4b\sqrt{1 - \mu'^2} \cos(\lambda' - \tau) + b^2(1 + \mu'))^2}{64} \cdot \frac{(1 + c^2 + \mu''(c^2 - 1))^2}{4 c^2} \\ &= \frac{(4(1 + c^2 + \mu''(c^2 - 1)) - 4bc\sqrt{1 - \mu''^2} \cos(\lambda'' - \tau) + b^2c^2(1 + \mu''))^2}{64 c^2} \end{aligned} \quad (2.17)$$

It is the square of a spherical harmonic of degree 1, its degree is then 2. We have proved that all the conformal mappings of the sphere are spectral and

of degree 2. A spectral model truncated at order N on the mapped sphere requires the collocation grid of an homogeneous model truncated at order N+2 to prevent the aliasing errors. Consequently, it is an economical way to build a clean variable resolution model. However, since the corresponding measure over the sphere is only at degree 2, we are very far from being able to approximate all the possible local increase of resolution, in particular we can easily see from the fact that the measure is the square of a spherical harmonic of degree 1 that there does not exist more than one area of concentration and one area of dilatation.

## 2.6 Interpretation of the transformation $z \rightarrow c(z+be^{i\tau})$

Let us define Q the point of the mapped sphere of colatitude  $\phi$  and longitude  $\tau$

$$\begin{aligned} \text{with } \cos \phi &= \frac{4(c^2-1) + b^2c^2}{\sqrt{(4(c^2-1) + b^2c^2)^2 + 16 b^2c^2}} \\ \sin \phi &= \frac{-4 b c}{\sqrt{(4(c^2-1) + b^2c^2)^2 + 16 b^2c^2}} \end{aligned} \quad (2.18)$$

If M is the point of coordinate  $(\mu'', \lambda'')$  ( $\mu'' = \cos \phi''$ ) then

$$F'(\lambda'', \mu'') = \left( \frac{\alpha^2-1}{2\alpha} \cos \gamma + \frac{\alpha^2+1}{2\alpha} \right)^2 \quad (2.19)$$

where  $\gamma$  is the arc QM and

$$\alpha = \frac{\sqrt{(4(c^2-1)+b^2c^2)^2 + 16 b^2c^2} + 4(1+c^2) + b^2c^2}{8 c}$$

By identification of (2.19) and (2.16), the transformation considered appears as an homothetic in the complex plane tangent to the mapped sphere at the point Q; it is the transformation introduced by Schmidt, the new feature here is that the pole of the collocation grid of the model has no longer to be at the pole of dilatation. That has one advantage: the problems introduced by the behaviour of the subgrid parametrization in the vicinity of the pole of the collocation grid (where the resolution of the physics is far more important than the resolution of the dynamics) would be removed to the periphery of the area of interest while in the centre of the area the resolution of the collocation grid would be quite homogeneous (assuming the pole of dilatation is put on the pseudo-equator). The above mentioned problems have to do more with the interpretation of parametrization output (e.g. rainfall fluxes, etc...) than with the interaction physics  $\leftrightarrow$  dynamics;

but in any case a quasi regular and quasi orthogonal grid on the real sphere in the centre of the area of interest appears to be a wishable feature for any operational post-processing package.

## 2.7 Particular cases

### 2.7.1 The pole of dilatation is the pole of the sphere

Then  $b=0$  and we have the transformation introduced by F. Schmidt and studied in Section 2.4.

### 2.7.2 The poles of extremum of dilatation are at the equator of the sphere

The colatitude  $\phi$  of Q is then equal to  $\pm \frac{\pi}{2}$

$$\cos \phi = 0$$

$$\sin \phi = 1, b < 0$$

$$\sin \phi = -1, b > 0$$

and  $\alpha = \frac{1 + \sqrt{1-c^2}}{c} \quad (0 < c \leq 1)$

This last case is of great practical interest because as already mentioned, the collocation grid is homogeneous in the middle of the area of maximum of resolution.

## 2.8 Conclusion

We have proved in this section that the only non trivial conformal transformations of the sphere are the homotheties in a given tangent plane, i.e. the transformations introduced by F. Schmidt. For a different, less algebraic and more geometric expression of this proof see Appendix A. In addition, we have also shown that the pole of the collocation grid has no longer to be the pole of maximum of resolution.

We have only studied the conformal transformations for two reasons. The first is that the shallow water equations on the transformed sphere are still very simple, the second comes from the fact that there is a priori no reasons to consider local interactions which are not isotropic. Nevertheless it is likely that some quasi conformal transformation are also spectral in the sense defined by F. Schmidt.

### 3. IMPLEMENTATION IN A SHALLOW-WATER EQUATIONS MODEL

#### 3.1 The shallow-water equations over the mapped sphere

The shallow water equations can be expressed in terms of a few differential operators :

$$\begin{aligned}\frac{\partial \xi}{\partial t} &= \nabla (\xi + f) \times \nabla \Delta^{-1} \xi - \nabla \cdot ((\xi + f) \nabla \Delta^{-1} \eta) \\ \frac{\partial \eta}{\partial t} &= \nabla (\xi + f) \times \nabla \Delta^{-1} \eta + \nabla \cdot ((\xi + f) \nabla \Delta^{-1} \xi) - \frac{1}{a^2} \Delta (\phi + K) \\ \frac{\partial \phi}{\partial t} &= \nabla \phi \times \nabla \Delta^{-1} \xi - \nabla \cdot (\phi \nabla \Delta^{-1} \eta)\end{aligned}\quad (3.1)$$

$$\text{with } K = a^2 [\nabla \Delta^{-1} \xi \cdot \nabla \Delta^{-1} \xi + \nabla \Delta^{-1} \eta \cdot \nabla \Delta^{-1} \eta + \nabla \Delta^{-1} \xi \times \nabla \Delta^{-1} \eta]$$

where  $\xi$  is the relative vorticity,  $\eta$  the divergence,  $\phi$  the geopotential,  $a$  the radius of the earth,  $f$  the planetary vorticity, and the notations for the differential operators are the same as in section 2,  $\Delta$  being the Laplacian operator and  $\Delta^{-1}$  its inverse. As a consequence of the equalities (2.3), we have :

$$\begin{aligned}\nabla \cdot (A \nabla B) &= \nabla' \cdot (A' \nabla' B') F' (\lambda', \mu') \\ \Delta^{-1} (A) &= \Delta'^{-1} \left( \frac{A'}{F'} \right)\end{aligned}\quad (3.2)$$

On the mapped sphere, the shallow-water equations take the following form :

$$\begin{aligned}\frac{\partial \alpha}{\partial t} &= \nabla' (\alpha F' + f) \times \nabla' \Delta'^{-1} \alpha - \nabla' \cdot ((\alpha F' + f) \nabla' \Delta'^{-1} \beta) \\ \frac{\partial \beta}{\partial t} &= \nabla' (\alpha F' + f) \times \nabla' \Delta'^{-1} \beta + \nabla' \cdot ((\alpha F' + f) \nabla' \Delta'^{-1} \beta) - \frac{\Delta'}{a^2} (\phi + F' K') \\ \frac{\partial \phi}{\partial t} &= [\nabla' \phi \times \nabla' \Delta'^{-1} \alpha - \nabla' \cdot (\phi \nabla' \Delta'^{-1} \beta)] F'\end{aligned}\quad (3.3)$$

with the same formal expression for  $K'$  as for  $K$ .

$$\text{where } \alpha = \frac{\xi}{F'} \text{ and } \beta = \frac{\eta}{F'} .$$

Originally, Schmidt chose  $(\phi/F')$  as a prognostic variable. We think that the choice of  $\phi$  as a prognostic variable is better for the following reason : the

geostrophic relation on the f-plane is  $\phi = f\psi$  where  $\psi$  is the stream function. It means that the geopotential and the stream function should have the same representation in the area of maximum of resolution, which is not achieved by the choice made by Schmidt.

### 3.2 Implementation in an explicit model

The transformation of a uniform resolution shallow-water equations model organized as the horizontal part of the ECMWF model into a non uniform one requires only three modifications in the computation on the collocation grid: the relative vorticity, the kinetic energy and the tendency of the geopotential, where the mapping factor is involved explicitly. In addition, the planetary vorticity has to be precomputed for each point of the collocation grid since its expression is no longer simple. The last technical modification concerns the number of points of the collocation grid NEW in the East-West direction and NNS in the North South direction. The inequalities between NEW and NNS and the degree N of the truncation are:

$$NEW - 1 > 3N + 2$$

$$2NNS - 1 < 3N + 2$$

instead of

$$NEW - 1 > 3N$$

$$2NNS - 1 > 3N$$

for an homogeneous model. When the number of points in East-West is a multiple of 3, there is no cost penalty. In addition, there are also some modifications to be included in the pre-processing and in the post-processing of the model to take into account that the model variables are defined on a transformed sphere.

### 3.3 The semi-implicit scheme

Let us consider the pseudo-divergence and geopotential equations written in the following symbolic form, the temporal scheme being a leap-frog scheme:

$$\begin{aligned} \beta(t+\Delta t) &= \beta(t-\Delta t) + 2 \Delta t F_{\beta} \\ \phi(t+\Delta t) &= \phi(t-\Delta t) + 2 \Delta t F_{\phi} \end{aligned} \tag{3.4}$$

where  $F_{\beta}$  and  $F_{\phi}$  are the explicit tendencies of the model. We follow Robert

et al. (1972) to implement an implicit treatment of the external gravity wave. We obtain the following system of equation for the pseudo-divergence and the geopotential at time  $t+\Delta t$ :

$$\begin{aligned}\beta(t+\Delta t) &= \beta(t-\Delta t) + 2 \Delta t [F_\beta + \frac{1}{2a^2} \Delta' [2\phi(t) - \phi(t+\Delta t) - \phi(t-\Delta t)]] \\ \phi(t+\Delta t) &= \phi(t-\Delta t) + 2 \Delta t [F\phi + \frac{1}{2} F' [2\beta(t) - \beta(t+\Delta t) - \beta(t-\Delta t)]]\end{aligned}\tag{3.5a}$$

which reduces to the two Helmholtz equations where only one has to be solved:

$$\begin{aligned}\beta - \frac{\Delta t^2 \bar{\phi}}{a^2} \Delta' (F' \beta) &= b_\eta \\ \phi - \frac{\Delta t^2 \bar{\phi}}{a^2} F' \Delta' (\phi) &= b_\phi\end{aligned}\tag{3.5b}$$

with  $b_\eta$  and  $b_\phi$  being functions of the known terms of 3.5a.

The problem is that the operators involved in the left hand side of 3.5b are no longer diagonal in spectral space (they admit the spherical harmonics of the geographical sphere as eigenvectors and not those of the mapped sphere). We have implemented this method in the case of a stretching at the northern pole, in which case the corresponding matrix of the operator is block-diagonal, each block corresponding to a given zonal wave number  $m$  being part diagonal. However it is not, as far as we know, so easy to achieve this if the pole of stretching is not the pole of the collocation grid. We have then looked for a simple solution:

The continuous equation of the external gravity wave is:

$$\begin{aligned}\frac{\partial \eta}{\partial t} &= - \frac{1}{a^2} \Delta \phi \\ \frac{\partial \phi}{\partial t} &= - \bar{\phi} \eta\end{aligned}\tag{3.6a}$$

and in the transform coordinates, it becomes:

$$\frac{\partial \beta}{\partial t} = - \frac{1}{a^2} \Delta' \phi$$

(3.6b)

$$\frac{\partial \phi}{\partial t} = - \bar{\phi} F' \beta$$

This last equation is formally the same as a gravity wave equation with a variable height  $\bar{\phi} F'$ . The maximum phase speed is obtained for the maximum value of the mapping factor, and we can implement the classical semi-implicit scheme but with an equivalent geopotential ( $\bar{\phi} \max(F')$ ). From the physical point of view, it means that we treat implicitly the external mode where the resolution is maximum and less implicitly elsewhere. However, in this latter case, the CFL criterion is less critical.

The important result is that this approach works and that the scheme is as stable as with the fully implicit treatment of the external gravity wave. No significant differences from the full scheme can be seen in the forecasts.

#### 3.4 Non-linear normal mode initialization

As for the semi-implicit scheme, in the general case we lose the separability between the wave numbers  $n$  and  $m$ .

The important practical point we show is that the Machenhauer, 1977 scheme implemented in the case of the pole of stretching at the northern pole still works (see Appendix B). Thus any initialization method based on the same definition of the slow manifold as for the Machenhauer algorithm will work. Furthermore an implicit method which does not require the explicit determination of the normal modes is conceptually more simple in the case of a variable mesh model and solves the problem of the storage of the normal modes (Temperton, 1985 or Sugi, 1986).

#### 4. NUMERICAL RESULTS

The experiments described in this section have been performed using a shallow-water equation model. The spatial discretisation uses the spectral technique and is achieved over the transformed sphere. In all the following experiments, the pole of stretching and the pole of the collocation (Gaussian) grid are located at the northern pole of the geographical sphere. The semi-implicit temporal scheme and the non linear normal-mode initialization process described in section 3 are used.



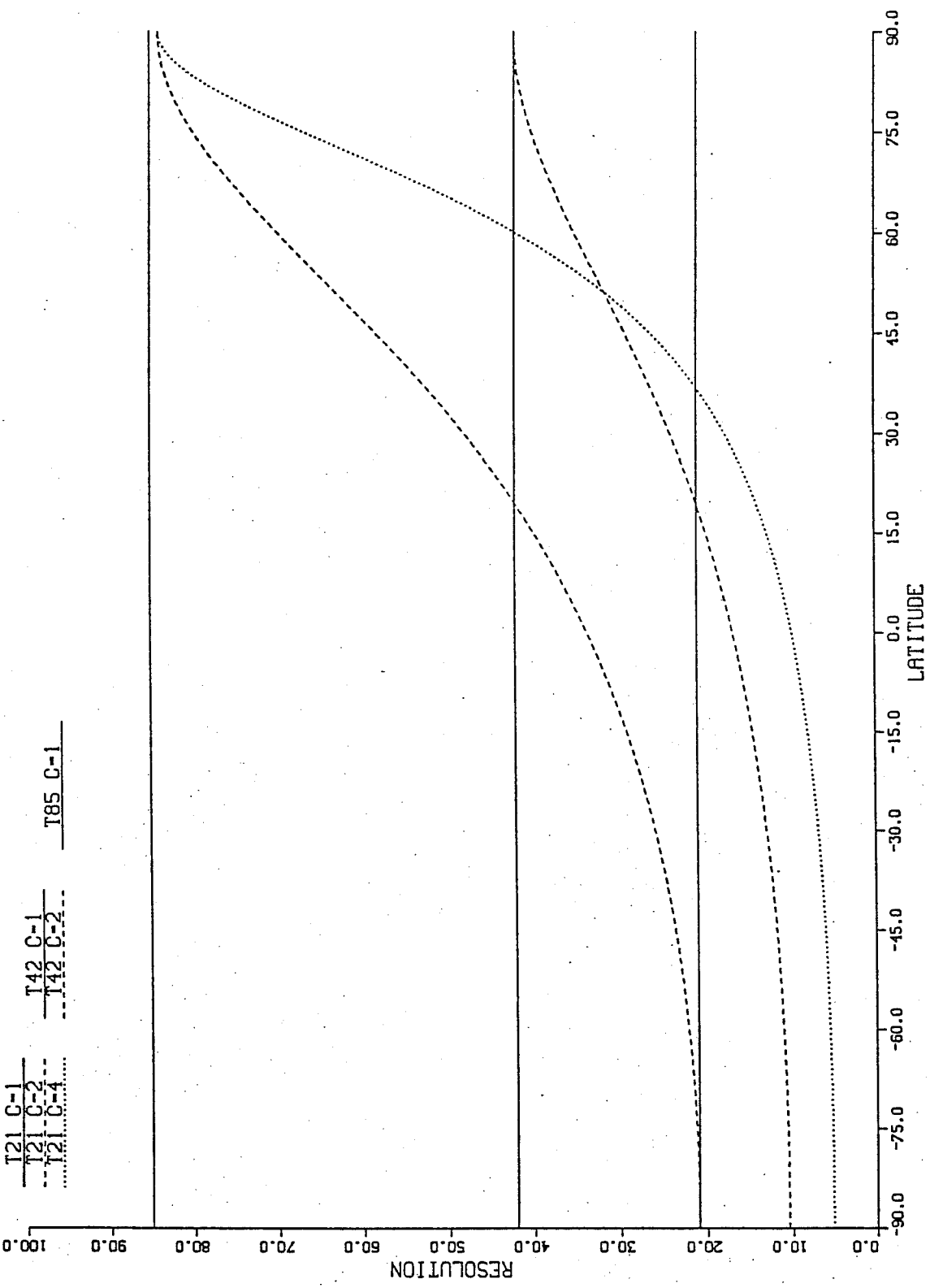


Fig. 3 Curves of resolution corresponding to:

- T21 C = 1, 2, 4
- T42 C = 1, 2
- T85 C = 1

in ordinates, maximum wave number of a triangular truncation.

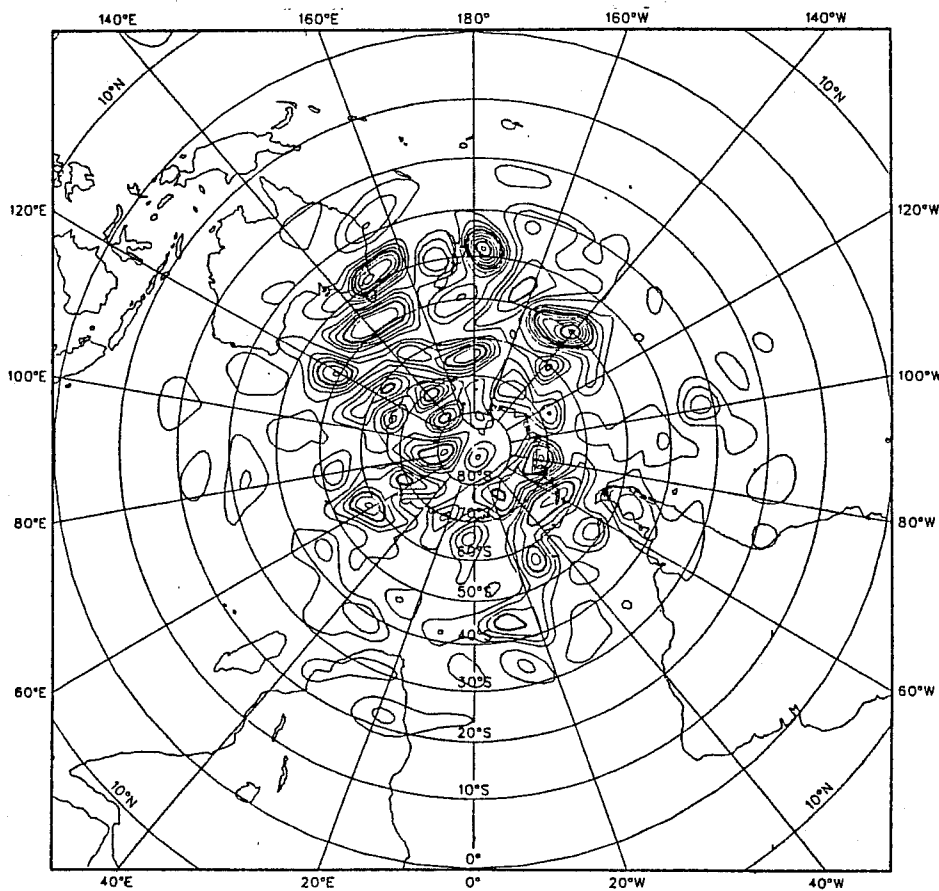
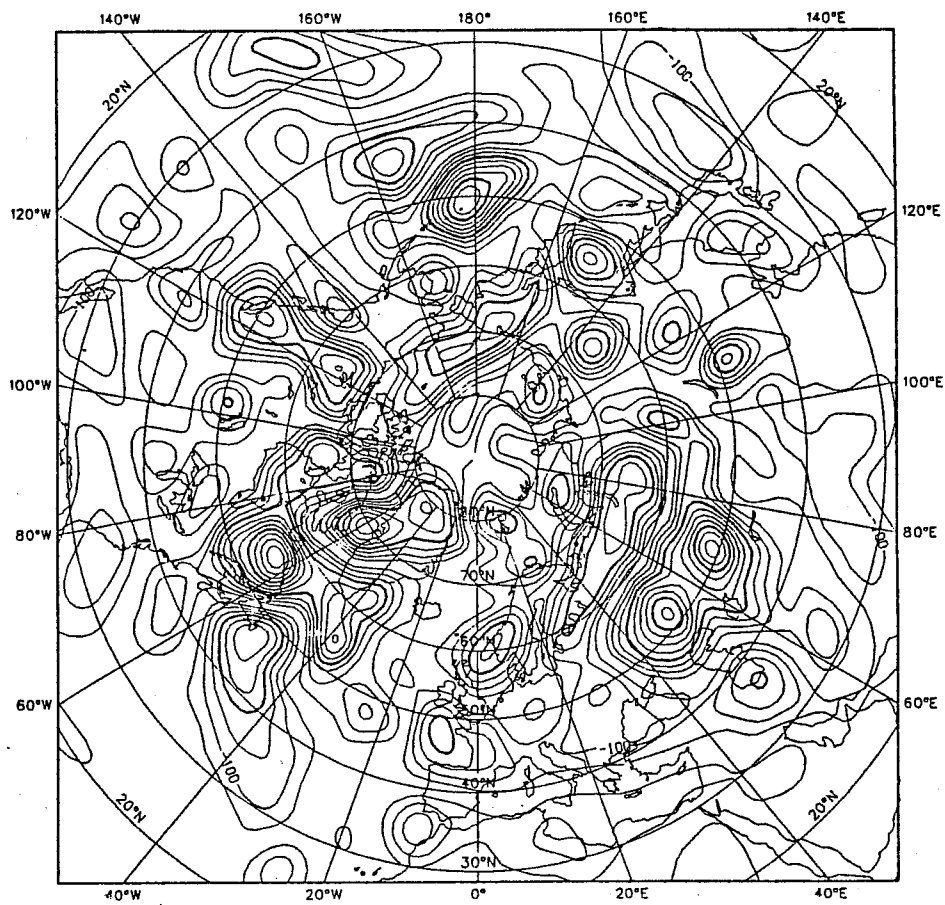


Fig. 4 Average over six consecutive days of the difference between the geopotential field (unit  $\text{m}^2\text{s}^{-2} = \text{J/kg}$ ) of the T21 c1 24 hour forecast and the T85 forecast taken as reference. Top is Northern Hemisphere and bottom Southern Hemisphere.

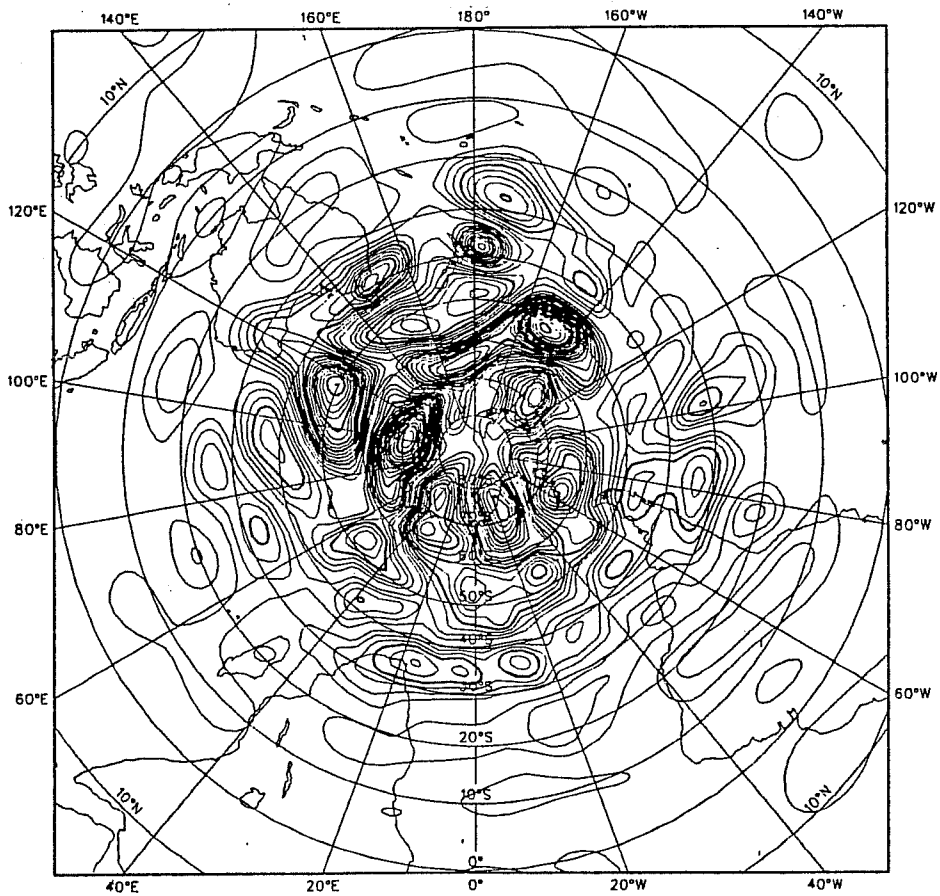
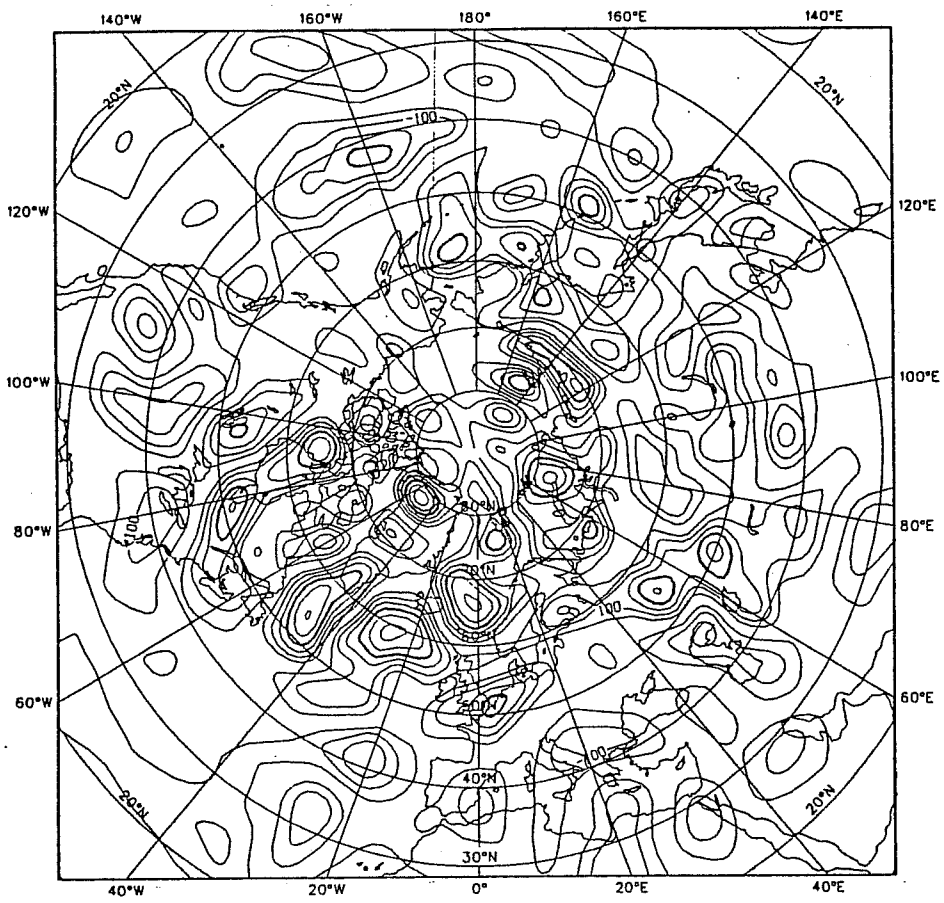


Fig. 5 Same as Fig. 4 but for the T21 c2 experiment.

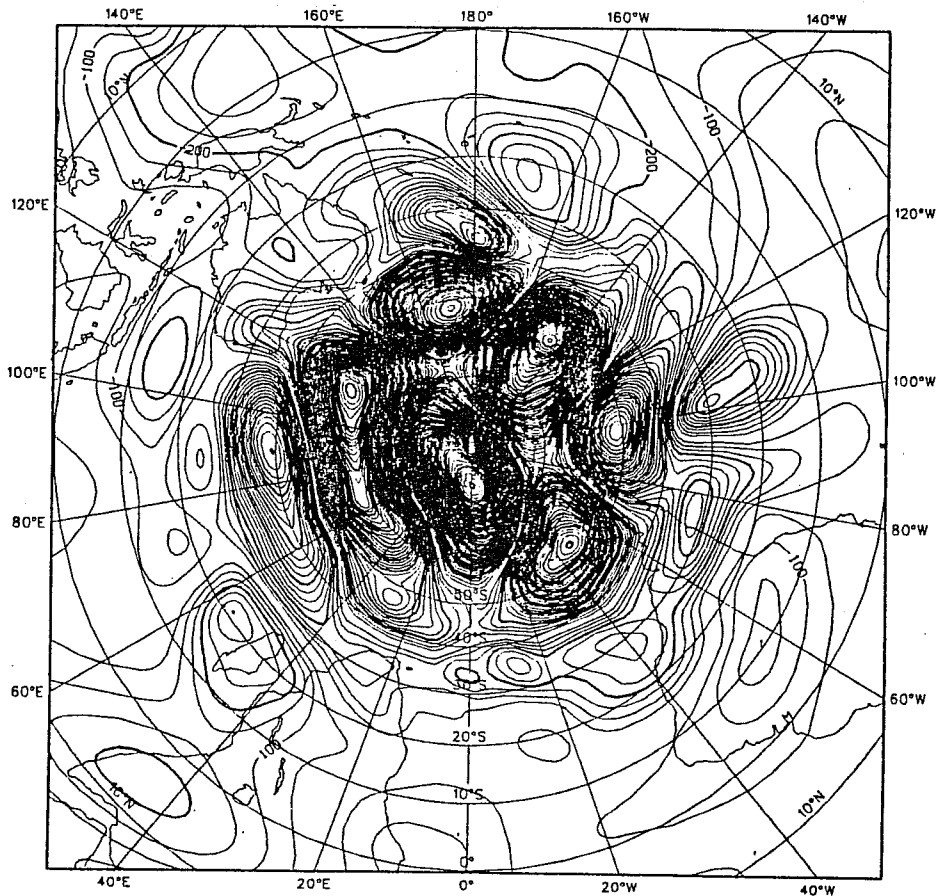


Fig. 6 Same as Fig. 4 but for the T21 c4 experiment.

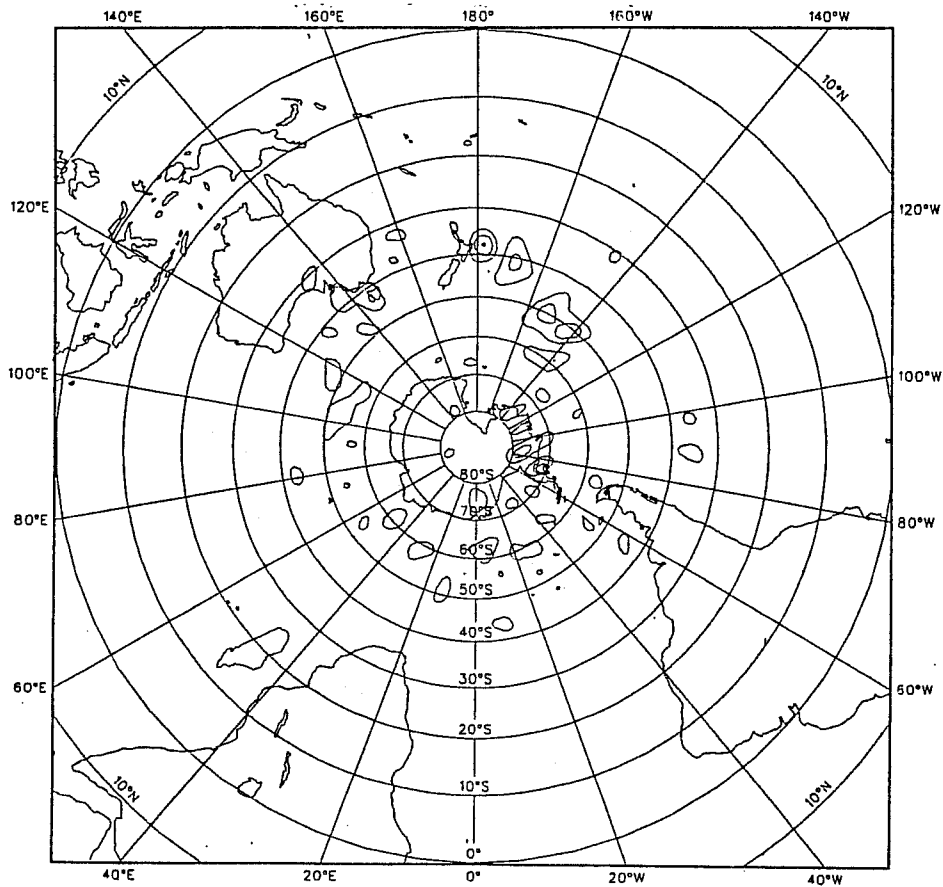
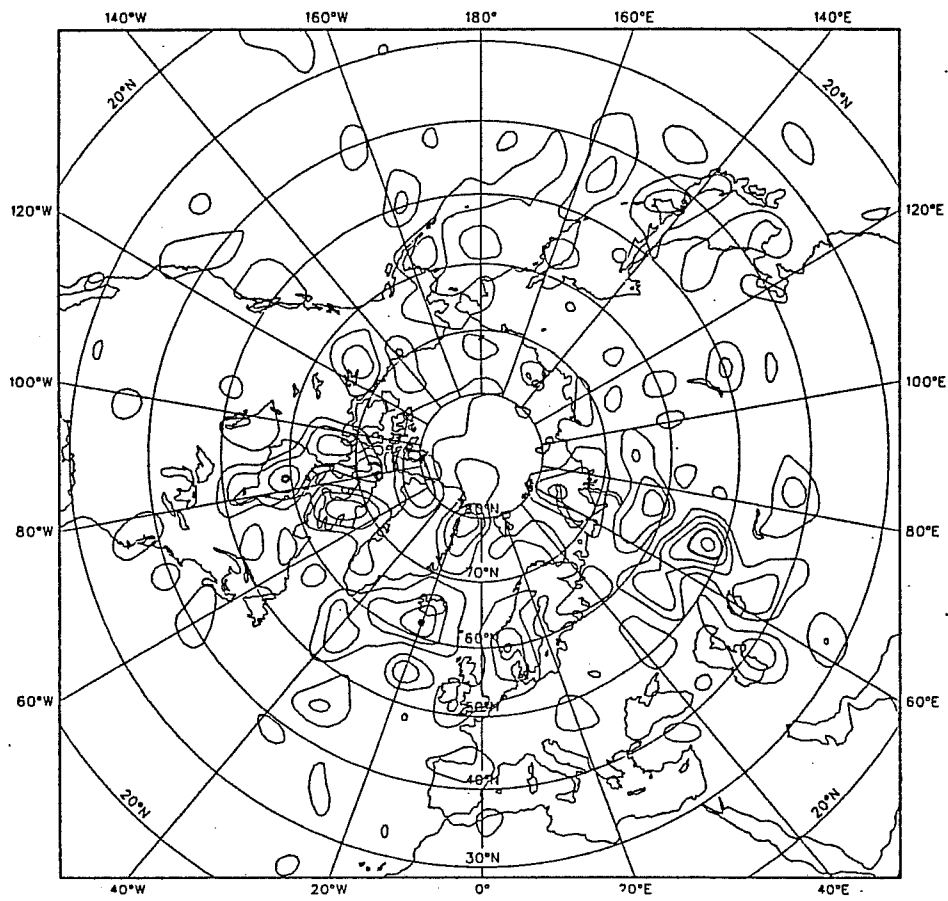


Fig. 7 Same as Fig. 4 but for the T42 c1 experiment.

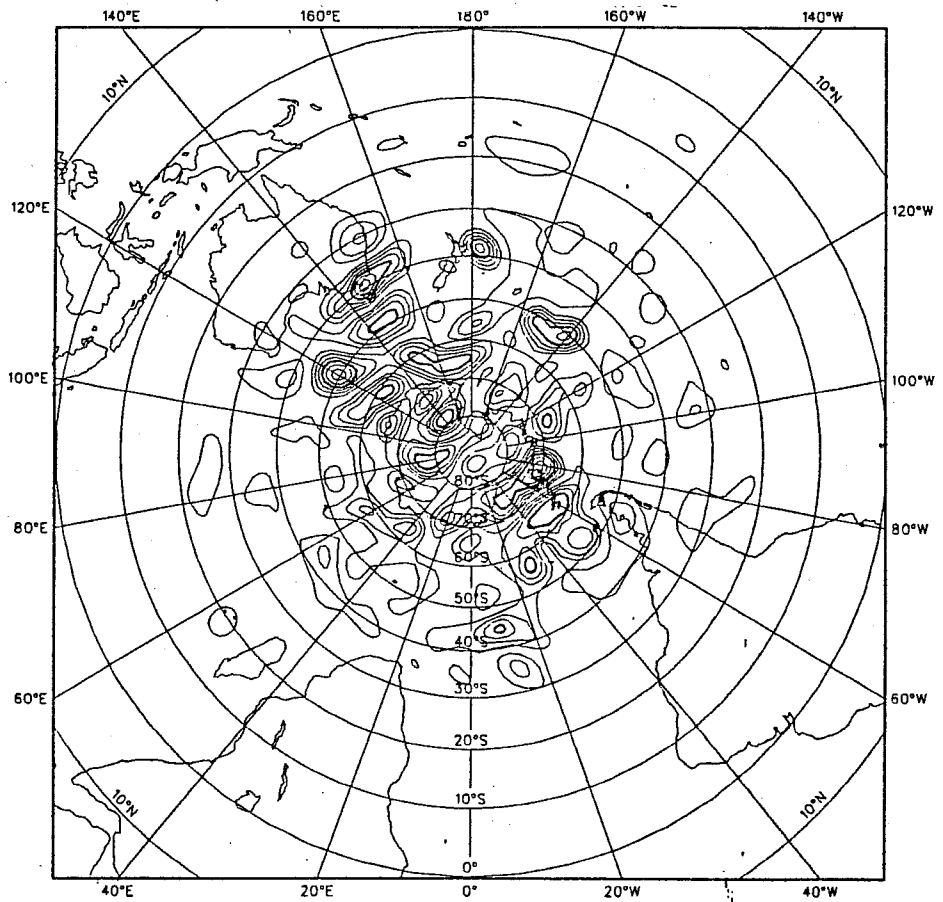
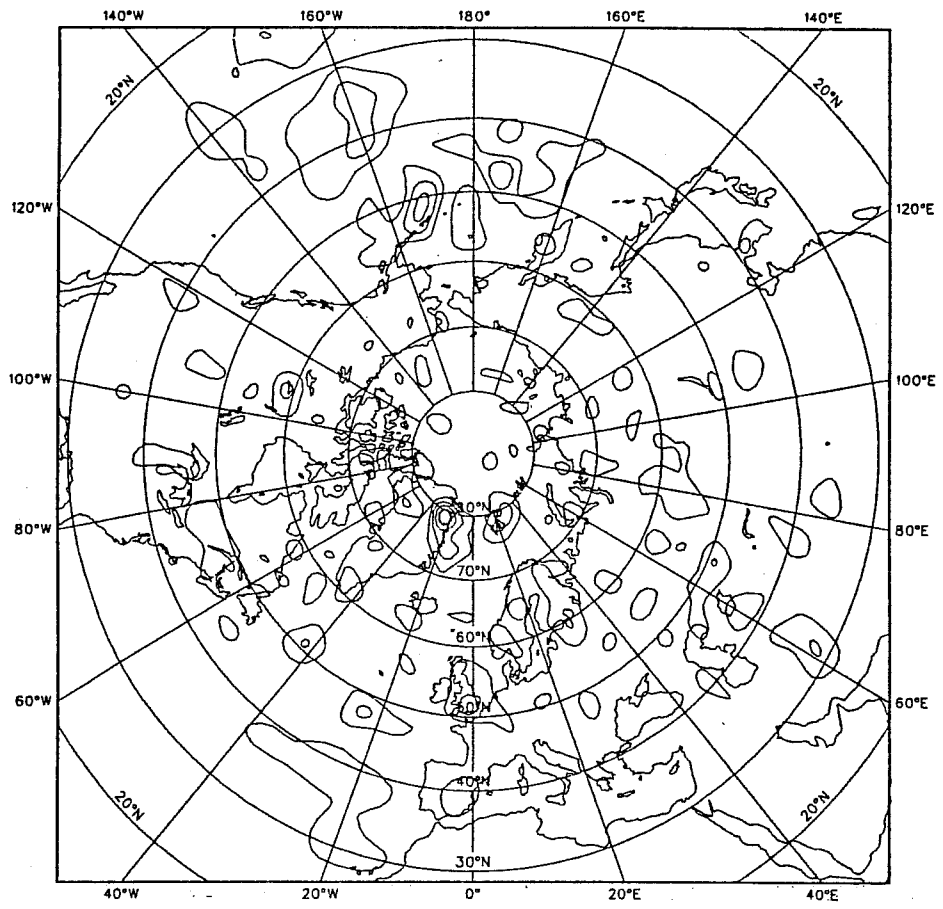


Fig. 8 Same as Fig. 4 but for the T42 c2 experiment.

#### 4.1 Meteorological results

We have performed a series of experiments using various values of the stretching factor  $c$  and of the degree  $N$  of the triangular truncation :

T21,  $c=1, 2, 4$

T42,  $c=1, 2$

T85,  $c=1$

The corresponding curves of resolution are presented on figure 3. At first sight, it seems that the area of maximum variation of resolution is quite close to the pole of maximum resolution. However this is a representation on the real sphere, unknown to our equations, while on the transformed sphere (the one that matters) the curve would be symmetrical i.e. the area of maximum change at the pseudo equator. We made six 24-hour forecasts starting from 00Z, 86-12-03, 86-12-04... 86-12-08. Figures 4, 5, 6, 7 and 8 show the average over the six cases of the mean differences between the forecast produced by the configurations of the model T21c1, T21,c2, T21c4, T42c1, T42c2 and the isotropic T85 which is taken as reference. The initial condition of each forecast is the operational ECMWF T106 analysis of vorticity, divergence and geopotential projected on the set of basis function of the given experiment and then followed by a non linear normal mode initialisation. The standard deviations maps were very similar to the mean maps for the matters we shall discuss below.

The main result is that the T21c2 (Figure 5) forecast is closer to the T42c1 (Figure 7) than to the T21c1 (Figure 4) in the northern hemisphere, which means that the gain in resolution is effective: In particular the large differences over the Rocky Mountains, the Aleutian area and the Caspian Sea vanish. In the North of the Atlantic Ocean, the improvement is negligible apart from the Hudson Bay where an important phase error has been removed. On the other hand, the T42c2 has a quality comparable to the T21c1 in the southern hemisphere: we lose resolution in the southern hemisphere but no more than was expected from the theory. It is important to point out that it is

not only the global quality which is the same but that even the local patterns are very similar: e.g. South of the Atlantic Ocean, Tasmania, and South of the Pacific Ocean.

We have only presented the results in terms of mean error. However, the root mean square maps and also maps for each individual case lead to the same conclusions. We have also made experiments on other dates (January 1987, May 1987 and June 1987) which confirm the above results.

We have made some further experiments at higher resolution : T63, c=1,2,4; T106, c=1,2; T133, c=1 and on other meteorological situations. The previous results are confirmed. In particular as the resolution increases, the shallow water equations become less sensitive to resolution (the initial conditions do not provide small-scale shocks) and the results of the different experiments become quite identical in the northern hemisphere. The important consequence is that the poor results of the T21c4 of the first set of experiments were not coming from the existence of non uniform resolution but from a lack of resolution in the southern part of the northern hemisphere, as can be seen on figure 3. This result is consistent with the fact that truncation 21 is a lower limit for a reasonable representation of synoptic scales.

These results are promising but they also have their limits. We have not studied the interactions between the horizontal discretisation and either the vertical one or the physical parametrisations. On the other hand we have not included any forcing like orography whose impact will a priori be enhanced with a better local resolution.

#### 4.2 Numerical considerations

The scheme has been proved to be stable in long-term runs (200 days) with a stretching factor in the range 1-4. For this, we used a Asselin (1972) time filter with a coefficient equal to 0.01 and also a slight diffusion, half the diffusion of the ECMWF T106 operational model. We have not investigated higher values of stretching for this question of stability, but, even if the non linear interaction are not described as in an isotropic model, there is a priori no reason to have a problem since there are no aliasing errors arising from the quadratic terms.



Some early results with no normal mode initialisation at the beginning of the forecast were found to be noisy in the area of maximum of resolution with high stretching factors (4-10). Although the problem has been cured with the introduction of the initialisation process, it was a strong indication that the gravity waves were trapped in the area of maximum of resolution. To study this problem, we integrated a degraded version of the model considering only the linear gravity wave equation 3.6. As initial conditions, we used an atmosphere at rest but with a geopotential field presenting a positive anomaly at the northern pole. In the isotropic case, the solution is analytic both in the continuous and the discretized case, the power spectrum being unchanged during the integration. In the stretched coordinate model, the equation is still linear but with coefficients varying in space and the shape of the power spectrum (with respect to the spherical harmonics of the mapped sphere) has no longer to be conserved. Numerical integrations show that as the wave propagates to the area of low resolution, the spectrum propagates to the high values of  $n$ , and when it reaches the degree of the truncation, it is associated with reflections in the physical space.

Obviously, this may be a problem for the implementation of the method, nevertheless we are optimistic for the following reasons :

- i) The problem is of the same nature as in the grid point case (Staniforth and Mitchell, 1978).
- ii) Only waves propagating in the radial direction are concerned by this problem.
- iii) The problem is maximum in the area of maximum change in resolution (and not the area of maximum resolution) and less important than in a limited area model where a wall condition is imposed.
- iv) Only the waves resolved in the area of maximum resolution and not in the area of minimum resolution are concerned.
- v) The local interactions being properly treated (the transformation is conformal), it is the boundary condition in spectral space imposed by the limitation of the truncation which creates the problem. It is

exactly of the same nature as the problem encountered in isotropic models of resolution between 50 km and 200 km where a part of the spectrum of the gravity waves is resolved but a more important part is not resolved.

We have studied the reflection of waves due to the variable mesh but we have not considered the possible problem of diffraction, which is minimized even if not suppressed by the conformality of the transformation. Another feature which has not been considered is the impact of the stretching on the stability of nonlinear equilibrium, a candidate for that study being the behaviour of modons in a vorticity equation model.

##### 5. POTENTIAL FOR NUMERICAL WEATHER PREDICTION (NWP) APPLICATIONS

Extension of the techniques described in Section 4 to primitive-equation models will obviously create no difficulty from the dynamical point of view (The problem of parametrization schemes with a validity extending over a whole range of horizontal resolutions will not be addressed here, despite our realisation of its crucial importance for operational NWP applications of the spectral transform technique). Thus it appears that the technique could be used as a viable alternative to three types of non homogeneous NWP systems: hemispheric models, nested systems starting from global (or hemispheric) and finishing with one or more limited area models (LAM) and, more surprisingly perhaps, LAM in stand-alone mode.

Before reviewing these three potential applications let us say something about the time stepping algorithm. In dynamical semi-implicit or split-explicit schemes the CFL condition will always be critical in the area of maximum resolution for the real sphere (or, in other words, in the area of strongest pseudo-winds on the mapped sphere). Thus the time step has to be chosen equal to the one corresponding to an homogeneous model of truncation  $cN$ . This is, in a certain sense, an unwelcome result: in areas of weak resolution (or weak pseudo-winds) one will have to use a too short time step for the local dynamics and thus pay in principle an unnecessary price for the flexibility of use of the spectral transformed sphere. However if one is interested in the results of the forecast only over a limited part of the earth the advocated solution will still be cheaper by a factor of about  $1/c$  than the one of an homogeneous global model. This gain is partly compensated by a loss of

accuracy that should however, according to results of Section 4, be far less important than the cost reduction.

But there is some hope that even the problem of the CFL dependency can be alleviated or even suppressed in some cases. Semi-Lagrangian techniques in a spectral model on the sphere are now more and more likely to become a reality in the coming years (Ritchie, 1987). Then the choice of the time step would depend on other considerations than the CFL criterion (physics, time truncation errors ....) and one could imagine it to become independent of the  $c$  factor if the latter is not too high ( $c < 2$  ?) or at least that the time step will not be the one dictated by the area of maximum resolution in case of high values of  $c$ . This shows that there is a mutually reinforcing interest of the two technical developments that spectral variable resolution models (SVRM) and semi-Lagrangian time stepping techniques represent.

Another less obvious advantage of the spectral transform technique can also be mentioned here: it allows, in purely spectral global problems, a strong reduction of  $N$  for a given maximum resolution and therefore puts a further delay to the time (in historical evolution) when the disadvantage of the  $N^3$  cost of Legendre transform will start being detrimental to spectral techniques against finite difference or finite element ones. On the other hand  $N^3$  is not an intrinsic property of the Legendre transform, there exist matrix multiplication algorithms whose asymptotic cost is  $N^{\log_2 7}$  and furthermore we have no proof that fast Legendre transforms do not exist.

### 5.1 SVRM as an alternative to hemispheric models

Hemispheric models are in fact global models (most of the time spectral ones) for which one assumes that the Southern Hemisphere is the exact symmetric of the Northern one. It is well known that, for forecasting in mid latitudes, the influence of a "wrong" equatorial boundary condition progressively deteriorates the quality of the forecasts, especially for the planetary ultra-longwaves (Sommerville, 1980, Arpe and Dittman, 1987) and that data-assimilation problems are paramount near the equator (Coiffier et al., 1987). For most applications a global model with a resolution divided by  $2^{1/3}$  offers a more physical and as cost-effective solution as the hemispheric model. But both these solutions are obviously superseded by a SVRM with polar axisymmetry and a rather small stretching factor ( $1 < c < \sim 1.5$ ), the

truncation being chosen to give the wanted local resolution at the latitude of interest (for Southern Hemispheric purposes one should of course replace  $c$  by  $1/c$ ). We shall not go further in the description of the advantages of such a solution since it was already done in the previous section.

## 5.2 SVRM as an alternative to nested systems

Nested systems (one-way or two-way interactive) are used in NWP to reach a high spatial resolution over an area of special interest without having to pay the price of such a resolution over the entire globe. Despite the use of efficient boundary relaxation techniques (Davies, 1976) there are still problems of brutal loss of information at the boundaries of the LAMs as well as problems of inward propagating gravity waves forced in the vicinity of the boundary by "physical" or orographic forcing. Such problems will have automatic counterparts in a SVRM system but with a surely less damaging intensity. Furthermore one SVRM means a single code while a nested system starting with a spectral global or hemispheric model and finishing with a LAM means at least two codes with all the maintenance problems created by such a duplication. Thus nested systems, where both the global and local forecasts are of practical interest, may be replaced by one SVRM with intermediate stretching factor ( $\sim 2 < c < \sim 3$ ) provided, of course, that the latter can be used with a semi-Lagrangian time stepping (otherwise the rise of the costs starts being too detrimental). Needless to say, one has, in this case, to make use of the rotation described in Section 2 in order to bring the maximum of resolution (and not necessarily the pole of the new grid) on the domain of interest. To give some order or magnitude we computed, merely as an example, that the coupled systems Emeraude/Peridot (Spectral T79/LAM 95x95 35 Km mesh) of the French Weather Service (DMN, Direction de la Meteorologie Nationale) would be roughly equivalent for its dynamical resolutions to a T127/ $c=3$  SVRM that would have a similar cost if an increase of about 4.3 in the time step could be obtained from quasi-Lagrangian techniques. The limit for cost effectiveness is below that value of 4.3 since the SVRM will suppress most of the problems associated with the LAM boundaries and since the "high resolution area" will have a larger extension than the one of the LAM. It might roughly be assumed to be between 2 and 3.

There is however one hidden drawback in the previous argumentation. The use of the SVRM technique would enforce the same vertical discretization for two

quite different problems, namely global synoptic forecasting and local mesoscale adaptation to local forcings. Operational practice shows that differences in the vertical structures are a welcome advantage of nested systems even if it causes some interpolation problems in the coupling. For example Emeraude and Peridot both have 15 levels but the cheapest, non degrading combination of both vertical grids would require 20 levels. This brings back, in a rough rule of thumb, the semi-Lagrangian threshold of efficiency around 3 if one also takes into account the increase in quality that will anyhow result of getting a better vertical resolution.

Of course all these very quantitative arguments will have to be qualified by clean experimental comparisons, with some a-priori edge given to the SVRM solution as a bonus for its "simplified maintenance" aspect.

### 5.3 SVRM as an alternative to LAM

All the arguments of Section 5.2 were of pure dynamical nature, without consideration of one of the disadvantages of the spectral technique: the diminished realism of the orographical forcing, owing to the necessity of exactly representing the orography in the truncated spectral space. It is known that this is not a too serious drawback in large scale models, but when going towards mesoscale forecasting the situation radically changes: the emphasis is then put on local adaptation to orography for the wind forecast and to the prediction of sensible weather for the thermodynamic variables (a domain where Gibbs phenomena are obviously damaging).

The consequences are that either the resolution should be increased everywhere (a costly solution) or that the stretching factor  $c$  should become even bigger than the values mentioned in 5.2 if one wishes to have a good mesoscale forecasting application of SVRM. However in the latter case an increase of  $c$  immediately creates (at equal costs) a degradation of the resolution at the antipodes of the area of interest, degradation that might become annoying if one also wishes to use the global forecast for general requirements.

One is therefore naturally lead to consider the application of SVRM as a limited area forecasting tool, i.e. the values outside a given area of interest being relaxed towards the results of a previous forecast performed by the same model but with a reasonable stretching factor (see 5.1 and 5.2).

When considering this possibility the first intuition is generally to consider that it will not be viable since the needed stretching factor for an efficient use would create too much distortion inside the area of interest. However, this is not the case, as will be shown below using an argumentation inspired by that of Schmidt (1982).

Let us assume a circular domain of interest of radius  $R$  (on the real sphere)  $R$  being expressed in radians. Once the point of maximum resolution has been put at the centre of the area, we are seeking, for a constant truncation, which stretching factor  $c$  will be maximising the minimal resolution inside the area of interest (i.e. on its edge). Such an optimum will obviously exist (provided  $R < \pi/2$ ) since stretching will first uniformly increase the resolution inside the circle of interest (as  $c \sim 1$ ) and ultimately lead to a vanishing resolution at the edge (as  $c \rightarrow \infty$ ). Let us see how this reads in mathematical terms.

The stretching factor on the edge of the domain is

$$s = \sqrt{F'} = [(1+c^2)+(1-c^2) \cos R]/2c$$

and  $\frac{ds}{dc} = 0$  gives  $c^2 = \frac{1+\cos R}{1-\cos R}$

and  $s = 1/\sin R$

But this simply means that, however small  $R$  might be, the optimum is always obtained when the edge of the area of interest is transformed as the equator of the mapped sphere, since

$$2 \operatorname{Arctan} \left( \sqrt{\frac{1+\cos R}{1-\cos R}} \tan \frac{R}{2} \right) = \frac{\pi}{2}$$

This is one more remarkable result of the Schmidt transform that makes it applicable to any "circular" LAM problem since the ratio  $r$  of the stretching factors between the centre of the area and its edge always remains inferior to two.

$$r = \sqrt{\frac{1+\cos R}{1-\cos R}} / (1/\sin R) = 1 + \cos R$$

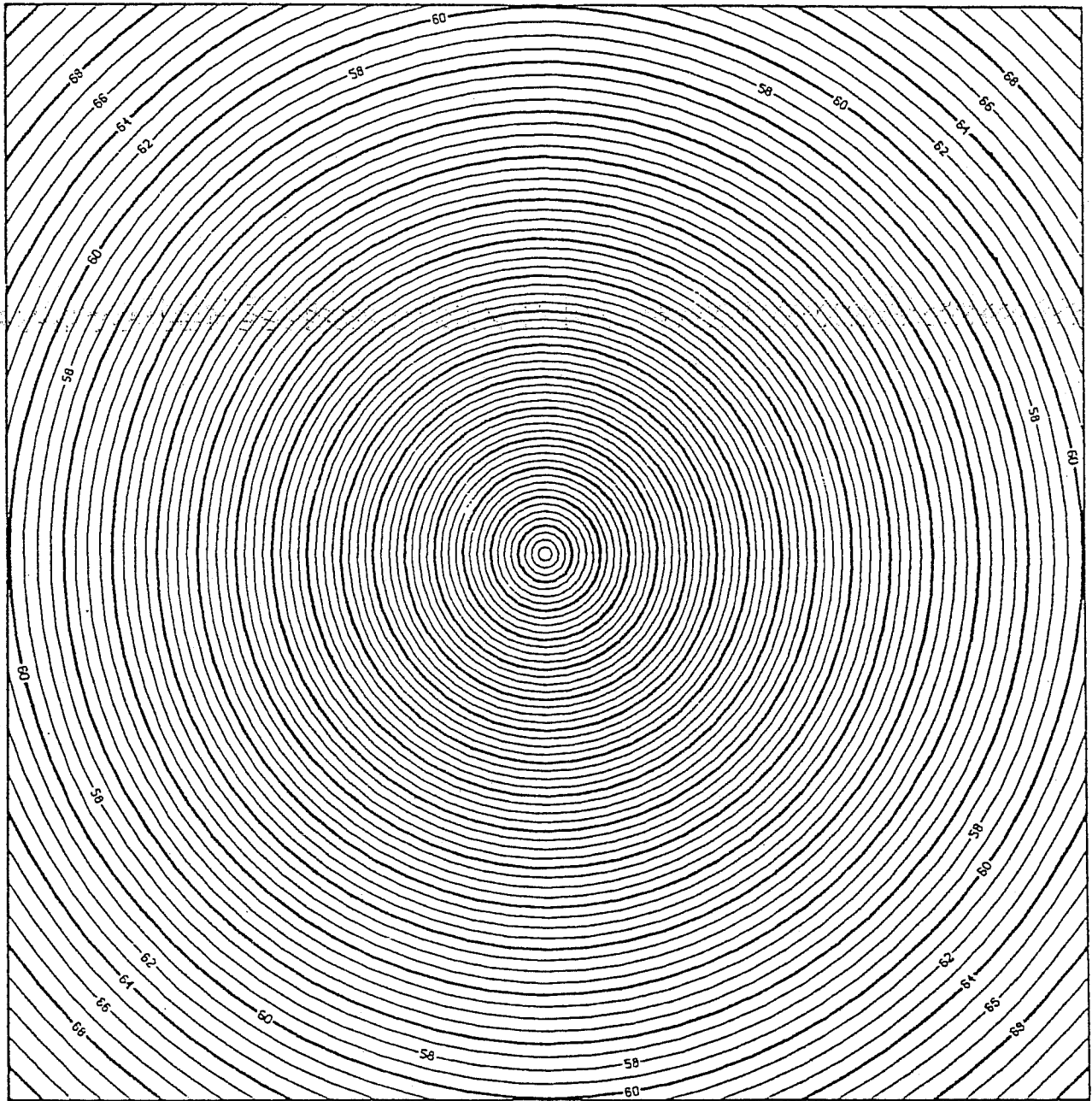


Fig. 9 Parallels of the collocation grid centred on the pole of stretching for a large value of  $c$ . Note that the ratio of the stretching between the centre and the edge (pseudo-Equator) is equal to two and is independent of the value of  $c$ .

In most applications  $R$  will be small so that  $r \approx 2$  (see Figure 9). This obviously reinforces the statement made at the beginning of 4.1 about the area of maximum varying resolution, equivalent to the brutal edge of a coupled LAM system but obviously far more satisfying in our case ("natura non fecit saltus").

In summary, in LAM applications of SVRM there will always be half of the grid points inside the area of interest and the other half outside it and there will never be more than a doubling of the resolution when going from the edge towards the centre of the area of interest. Furthermore, going back to the orography problem mentioned earlier, the choice of the "edge-resolution" as dynamically equivalent to the one of a classical LAM will give an improved orographical definition over a good part of the domain, around its centre. And the advantages of a spectral solution against a finite difference one will partly compensate for the "waste" of half the degrees of freedom in the model so that the solution will remain reasonably efficient, provided once again, that a semi-Lagrangian improvement on the time step of the order of 3 can be reached. This is not, in our mind, too detrimental a figure and we thus think that a carefully balanced use of the options described in 5.1, 5.2 and 5.3 should be able to offer a cost effective alternative to any of today's existing NWP systems.

## 6. CONCLUDING REMARKS

In this paper we have shown that the spectral conformal transform introduced by Schmidt (1977) is the only non trivial one of its kind when going from sphere to sphere. We also indicate that practical applications of this technique should be thought in terms of classical spectral techniques applied to the mapped sphere (rather than changing equations on the real sphere). This, for instance, enables a dissociation between the areas of maximum and minimum resolution and the poles of the collocation grid.

The results of several experiments with shallow water equations are conclusive enough to give confidence that the method can be applied to operational NWP problems in a not too distant future. Some rather preliminary thoughts about possible strategies of use were outlined. In fact the last two of them are part of the plans at the French Weather Service (DMN) to develop a new forecasting system oriented towards short range global synoptic and local



mesoscale features; the first one (the only one tested here in the shallow water version) could easily be applied to medium range global forecasting.

These types of application will require progress in at least two connected areas: parametrization schemes with a wider range of validity in terms of horizontal scales and semi Lagrangian time stepping. There is, however, no reason to fear that such progress cannot be achieved to a sufficient extent in the coming years and we thus foresee that the "F. Schmidt transform" will soon be mentioned not only for its remarkable mathematical properties but also for its unifying role in operational NWP problems.

#### Acknowledgements

The authors thank A. Simmons for the part he took in the work and B. Machenauer for discussions. Suggestions from P. Bougeault, J. Coiffier, F. Delsol, Y. Durand, M. Jarraud, M. Rochas in the framework of a working group to initiate the project Action de Recherche Petite Echelle Grande Echelle (ARPEGE) of the French Weather Service are also acknowledged. S. Arnoux checked (and corrected) the proof of section 2. M. Simpson typed very carefully the manuscript. We thank Andrew Staniforth, whose contribution greatly improved the original paper.

#### APPENDIX A

##### TRIGONOMETRIC INTERPRETATION OF THE RESULTS OF SECTION 2

The results of this paper can be interpreted in a more geometric (or rather trigonometric) sense.

Let us first consider the transform introduced by Schmidt (1977) who, surprisingly enough, never mentioned its obvious geometrical interpretation (in its most simple analytical form the transform reads  $\tan \frac{\phi'}{2} = c \tan \frac{\phi}{2}$  when going from the real ( $\phi$ ) to the pseudo ( $\phi'$ ) sphere)

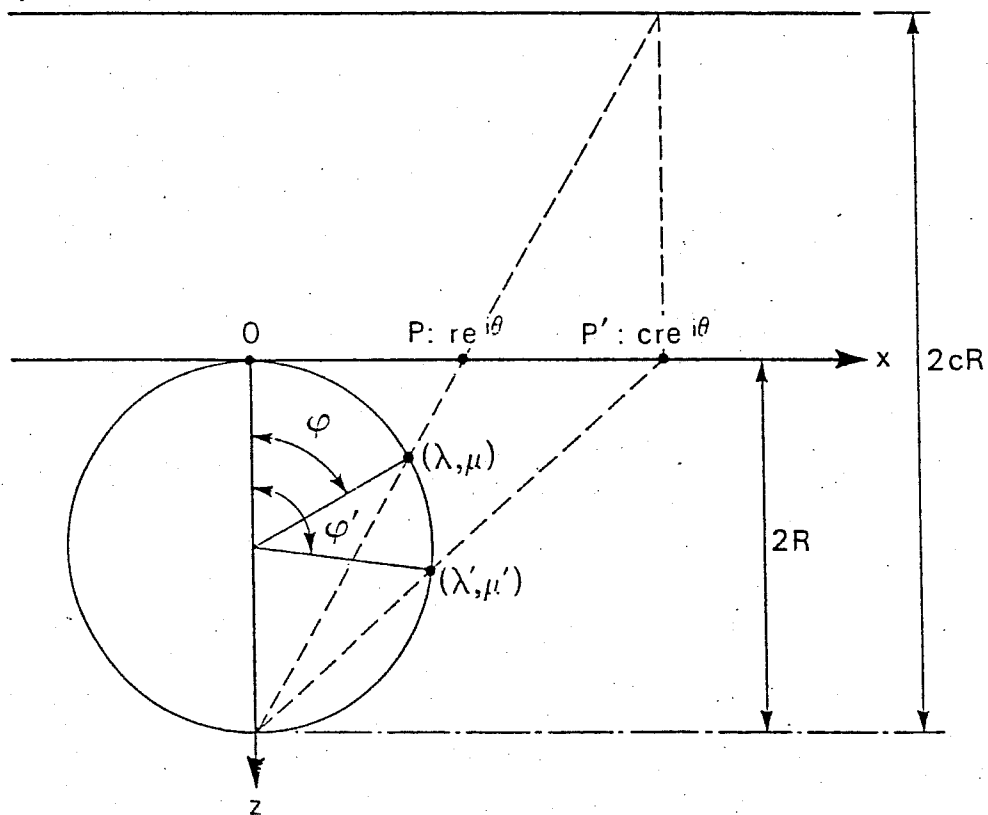


Fig. 10 The transformation associated to a magnification in the complex plane.

Figure 10 has been drawn in the  $Oxz$  plane but a rotation around the  $Ox$  axis in the  $Oxy$  plane after going from  $P'$  to  $P$  (rotation after homothetic) would, of course, keep the spectral and conformal properties of the transform and the result in the complex plane  $Oxy$  would be

$$x' + iy' = (\alpha + i\alpha')(x + iy)$$

The crucial point, if one wants to abandon the privileged role of the  $Oz$  axis (i.e. to rotate the points of maximum and minimum resolution) is that the relation

$$\tan\left(\frac{\phi}{2} + \frac{\phi_0}{2}\right) = \frac{\tan\frac{\phi}{2} + \tan\frac{\phi_0}{2}}{1 - \tan\frac{\phi}{2} \cdot \tan\frac{\phi_0}{2}} \quad \text{is homographic in } \tan\frac{\phi}{2}$$

Let us, for the time being, stay in the  $Oxz$  plane, that is the complex numbers in the  $Oxy$  plane will keep real values.

A rotation by an angle  $\phi_0$  of the axis connecting the points of maximum and minimum resolution can readily be converted into an homographic transform along the  $Ox$  axis of the  $Oxy$  plane. Using the trigonometric formula just above and setting  $\tan \frac{\phi_0}{2} = -\frac{1}{c}$  one gets

$$X = \frac{cx - 1}{x + c} \quad (\text{A.1})$$

We still have two things to show to come to result equivalent to the one of Section 2: first that the relation (A.1) remains valid when going to the full complex plane and second that all the degrees of freedom of the most general homographic complex transform can be expressed by a combination of (A.1) and of homotheties/rotations.

Let us first prove the second point. Depending on the arbitrary choice of the  $Ox$  axis in the  $Oxy$  plane we can choose  $c$  real without loss of generality.

Thus one homothetic/rotation before and after (A.1) will lead to

$$\frac{X}{\alpha + i\alpha'} = \frac{c \frac{x}{\beta + i\beta'} - 1}{\frac{x}{\beta + i\beta'} + c} \Rightarrow X = \frac{c(\alpha + i\alpha')x - (\alpha + i\alpha')(\beta + i\beta')}{x + c(\beta + i\beta')} \quad (\text{A.2})$$

that possesses 5 of the 6 degrees of freedom of the general complex homographic transform, the last one being the one we just removed ( $c$  real).

Finally, we study the equivalent of (A.1) with  $X+iY$  replacing  $X$  and  $x+iy$  replacing  $x$ .

We obtain:

$$X = \frac{(cx-1)(x+c) + cy^2}{(x+c)^2 + y^2} \quad (\text{A.3})$$

$$\text{and } Y = \frac{(c^2+1)y}{(x+c)^2 + y^2} \quad (\text{A.4})$$

Let us compare this result with a rotation around the 0y axis in the three dimensional space.

$$\text{From } x, y \text{ we get } \phi, \lambda : \cos \phi = \frac{1-x^2-y^2}{1+x^2+y^2} \quad \sin \phi = \frac{2\sqrt{x^2+y^2}}{1+x^2+y^2}$$

$$\cos \lambda = \frac{x}{\sqrt{x^2+y^2}} \quad \sin \lambda = \frac{y}{\sqrt{x^2+y^2}}$$

Thus on the sphere (nondimensionalized by its diameter) and after an inverse stereographic projection,

$$2x' = \sin \phi \cos \lambda = 2x/(1+x^2+y^2)$$

$$2y' = \sin \phi \sin \lambda = 2y/(1+x^2+y^2)$$

$$2z' = \cos \phi = (1-x^2-y^2)/(1+x^2+y^2)$$

The rotation has  $\phi_0$  for angle with  $\tan \frac{\phi_0}{2} = -\frac{1}{c}$   
 i.e.  $\cos \phi_0 = \frac{c^2-1}{c^2+1}$  and  $\sin \phi_0 = \frac{-2c}{c^2+1}$

The rotation acts in  $x'z'$  to get  $X'Z'$  with  $Y'=y'$

$$2X' = [(2x)(c^2-1) - (1-x^2-y^2)(2c)]/[(1+x^2+y^2)(c^2+1)]$$

$$2Y' = [(2y)(c^2+1)]/[(1+x^2+y^2)(c^2+1)]$$

$$2Z' = [(1-x^2-y^2)(c^2-1) + (2x)(2c)]/[(1+x^2+y^2)(c^2+1)]$$

And, going back to the tangent plane OXY by stereographic projection:

$$X = \frac{2X'}{1+2Z'} = \frac{(cx-1)(x+c) + cy^2}{(x+c)^2 + y^2} \quad (\text{A.5})$$

$$Y = \frac{2Y'}{1+2Z'} = \frac{(c^2+1)y}{(x+c)^2 + y^2} \quad (\text{A.6})$$

that is Equations A.3 and A.4; q.e.d.

APPENDIX B

NON-LINEAR NORMAL MODE INITIALISATION

We consider the shallow-water equations 3.3 linearized in the vicinity of a state of rest:

$$\begin{aligned} \frac{\partial \alpha}{\partial t} &= \nabla f \times \nabla \Delta^{-1} \alpha - \nabla \cdot (f \nabla \Delta^{-1} \beta) \\ \frac{\partial \beta}{\partial t} &= \nabla f \times \nabla \Delta^{-1} \beta + \nabla \cdot (f \nabla \Delta^{-1} \alpha) - \frac{1}{a^2} \Delta \phi \\ \frac{\partial \phi}{\partial t} &= - \bar{\phi} F'(\lambda', \mu') \beta \end{aligned} \tag{B.7}$$

There are two differences between this set of equations and the corresponding set over the geographical sphere:

- i)  $f$ , the planetary vorticity, is not equal to  $2\Omega\mu'$  as in the isotropic case.
- ii)  $F'(\lambda', \mu')$  is introduced in the equation of evolution of the geopotential.

It has to be noted that, in general, we lose the separability between latitude and longitude; and in the particular case where the pole of stretching is at the northern pole, we lose only the separability between the symmetric and antisymmetric modes with respect to the equator.

The following developments are valid in this latter case. We make the further approximation:

$$f = 2\Omega (f_0 + f_1 \mu) \tag{B.8}$$

which is valid if the minimum of resolution over the geographical sphere is more than T2 (e.g. with a truncation at degree 21 over the mapped sphere, the stretching factor has to be less than 10).

The mapping factor is a polynomial of degree 2 in  $\mu'$ :

$$F'(\lambda', \mu') = F'_0 + F'_1 \mu' + F'_2 \mu'^2 \quad (\text{B.9})$$

Thus the equation B.7 reads:

$$\begin{aligned} \frac{\partial \alpha}{\partial t} &= 2\Omega \left[ -f_1 \frac{\partial \Delta^{-1} \alpha}{\partial \lambda} - f_0 \beta - f_1 \mu \beta - (1-\mu^2) f_1 \frac{\partial \Delta^{-1} \beta}{\partial \mu} \right] \\ \frac{\partial \beta}{\partial t} &= 2\Omega \left[ -f_1 \frac{\partial \Delta^{-1} \beta}{\partial \lambda} + f_0 \alpha + f_1 \mu \alpha + (1-\mu^2) f_1 \frac{\partial \Delta^{-1} \alpha}{\partial \mu} \right] - \frac{1}{a^2} \Delta \phi \quad (\text{B.10}) \\ \frac{\partial \phi}{\partial t} &= -\bar{\phi} \beta (F'_0 + F'_1 \mu + F'_2 \mu^2) \end{aligned}$$

We introduce the following non-dimensionalization of the equations in order to:

- i) have a real operator
- ii) improve the conditioning of the eigenvalue problem.

$$\begin{aligned} A &= \frac{\alpha}{2\Omega} \\ B &= -i \frac{\beta}{2\Omega} \\ C &= \frac{1}{2\Omega a} \frac{1}{\sqrt{F'_0 \bar{\phi}}} |\Delta|^{\frac{1}{2}} \phi \\ \tau &= \frac{2\Omega t}{i} \end{aligned} \quad (\text{B.11})$$

The equations become:

$$\begin{aligned} \frac{\partial A}{\partial \tau} &= -i f_1 \frac{\partial \Delta^{-1} A}{\partial \lambda} + f_0 B + f_1 \mu B + (1-\mu^2) f_1 \frac{\partial \Delta^{-1} B}{\partial \mu} \\ \frac{\partial B}{\partial \tau} &= -i f_1 \frac{\partial \Delta^{-1} B}{\partial \lambda} + f_0 A + f_1 \mu A + (1-\mu^2) f_1 \frac{\partial \Delta^{-1} A}{\partial \mu} + \frac{\sqrt{F'_0 \bar{\phi}}}{2\Omega a} |\Delta|^{\frac{1}{2}} C \\ \frac{\partial C}{\partial \tau} &= \frac{\sqrt{\bar{\phi} F'_0}}{2\Omega a} |\Delta|^{\frac{1}{2}} \left[ \left[ 1 + \frac{F'_1}{F'_0} \mu + \frac{F'_2}{F'_0} \mu^2 \right] B \right] \end{aligned} \quad (\text{4.12})$$

We express A, B and C in spherical harmonics, and since we have obviously a separation between the different zonal wave numbers m, for a given m we have:

$$\begin{aligned} \frac{\partial}{\partial \tau} \sum_{n=m}^{+\infty} A_n^m Y_n^m &= \sum_{n=m}^{+\infty} Y_n^m [K_n^m f_1 A_n^m + f_0 B_n^m + q_n^m f_1 B_{n+1}^m + p_n^m f_1 B_{n-1}^m] \\ \frac{\partial}{\partial \tau} \sum_{n=m}^{+\infty} B_n^m Y_n^m &= \sum_{n=m}^{+\infty} Y_n^m [K_n^m f_1 B_n^m + f_0 A_n^m + q_n^m f_1 A_{n+1}^m + p_n^m f_1 A_{n-1}^m \\ &+ \varepsilon_n C_n^m] \end{aligned} \quad (\text{B.13})$$

$$\begin{aligned} \frac{\partial}{\partial \tau} \sum_{n=m}^{+\infty} C_n^m Y_n^m &= \sum_{n=m}^{+\infty} \varepsilon_n Y_n^m [B_n^m (1 + (D_n^{m2} + D_{n+1}^{m2}) \frac{F'_2}{F'_0}) \\ &+ B_{n+1}^m D_{n+1}^m \frac{F'_1}{F'_0} + B_{n-1}^m D_n^m \frac{F'_1}{F'_0} \\ &+ B_{n+2}^m D_{n+1}^m D_{n+2}^m \frac{F'_2}{F'_0} + B_{n-2}^m D_{n-1}^m D_n^m \frac{F'_2}{F'_0}] \end{aligned}$$

with  $\varepsilon_n = \frac{\sqrt{n(n+1)}}{\sqrt{\phi F'_0}} \frac{1}{2\Omega a}$

$$D_n^m = \sqrt{\frac{n^2 - m^2}{4n^2 - 1}}$$

$$K_n^m = -\frac{m}{n(n+1)} \quad k_0^0 = 0$$

$$p_n^m = D_n^m \frac{n+1}{n} \quad p_0^0 = 0$$

$$q_n^m = D_{n+1}^m \frac{n}{n+1}$$

We solve the eigenvalue problem defined by B.13 for a given m and obtain the normal modes of the model. We are then able to use the Machenhauer non-linear normal-mode initialisation algorithm. Nevertheless, it has to be pointed out that the crucial problem of the storage of the normal modes is now worse:

- i) as we have lost the separability between symmetric and antisymmetric modes, the storage requirements are multiplied by two.
- ii) the scalar product for which the modes are orthogonal corresponds to a uniform measure over the geographical sphere and is no longer diagonal over the mapped sphere. The practical consequence is that we need to store both the expansion of the spherical harmonics in terms of the normal modes and the normal modes in terms of the spherical harmonics. The storage requirements are then multiplied by another factor of 2.

## References

- Arpe, K. and Dittman, E., 1987: Comparison of forecast performances up to 5 days with a global and a hemispheric model. *Beitz.Phys.Atmos.* 60, 193-210.
- Asselin, R., 1972: Frequency filter for time integrations. *Mon.Wea.Rev.*, 100, p 487-490.
- Cartan, H., 1961: *Téorie élémentaire des fonctions analytiques d'une ou plusieurs variables complexes.* Hermann, publisher, Paris. 231 pp.
- Coiffier, Ernie, Geleyn, Clochard, Hoffman, Dupont, 1987: The operational hemispheric model of the French Meteorological Service, *Jour.Met.Soc.Japan.*, NWP Symposium special issue, 1987, pp 337-345.
- Davies, H.C., 1976: A lateral boundary formulation for multi-level prediction models. *Quart.J.R.Met.Soc.*, 102, 405-418.
- Jarraud, M., and Simmons, A., 1983: The spectral technique. Report of ECMWF Seminar, 1983: Numerical techniques for weather prediction. 2, 1-60.
- Machenauer, B., 1977: On the dynamics of gravity oscillations in a shallow-water model with applications to normal mode initialization. *Contrib.Atmos.Phys.* 50, 253-271.
- Ritchie, H., 1987: Semi Lagrangian advection on a Gaussian grid. *Mon.Wea.Rev.*, 115, 608-619.
- Robert, A.S., Hendersen, J., Turnbull, C., 1972: An implicit time integration scheme for baroclinic models of the atmosphere. *Mon.Wea.Rev.*, 100, 329-335.
- Saff, E.B. and A.D. Snider, 1976: *Fundamentals of complex analysis*, Prentice Hall.
- Sharma, O.P., Upadhyaya, H., Braine-Boussaine, Th., Sadourny, R. Experiments on Regional Forecasting using a Stretched Coordinate General Circulation Model. *Jour.Met.Soc.Japan.*, NWP Symposium special issue, 1987, pp 263-271.
- Schmidt, F., 1977: Variable fine mesh in spectral global model. *Beitz.Phys.Atmosph.* 50, 211-217.
- Schmidt, F., 1982: Cyclone tracing. *Beitr.Phys.Atmosph.* Vol. 55 No. 4, 335-357.
- Sommerville, R.C.J., 1980: Tropical influences on the predictability of ultra long waves. *J.Atmos.Sci.*, 37, 1141-1156.
- Staniforth, A. and Mitchell H., 1978: A variable resolution finite element technique for regional forecasting with the primitive equations. *Mon.Wea.Rev.*, 106, 439-447.
- Sugi, M., 1986: Dynamic normal mode initialization. *Jour.Met.Soc.Jap.* 64, 623-636.
- Temperton, C., 1985: Implicit normal mode initialization. 1935 World Climate Research Program Report on research activities in atmospheric and oceanic modelling, World Met. Org., p 1.21.